Repetitive Control for Lur'e-Type Systems: Application to Mechanical Ventilation

Joey Reinders[ID], Mattia Giaccagli[ID], Bram Hunnekens[ID], Daniele Astolfi[ID], Tom Oomen[ID], *Senior Member, IEEE*, and Nathan van de Wouw[ID], *Fellow, IEEE*

Abstract— **Repetitive control (RC) has shown to achieve superior rejection of periodic disturbances. Many nonlinear systems are subject to repeating disturbances. The aim of this article is to develop a continuous-time RC design with stability guarantees for nonlinear Lur'e-type systems. Approximate output tracking is achieved by combining an internal model, consisting of a finite number of linear oscillators with frequencies at the reference frequency and at its multiples, with a stabilizer that guarantees a convergence property of the closed-loop system. The developed RC approach is applied to a nonlinear mechanical ventilation system for intensive care units (ICUs), which can be modeled as a Lur'e-type system. The experimental study confirms that the RC scheme is able to successfully follow the desired target pressure profile to properly support the ventilation needs of an adult patient.**

Index Terms— **Circle criterion, convergent systems, harmonic regulation, Lur'e-type system, mechanical ventilation, medical applications, nonlinear output regulation, repetitive control (RC).**

I. INTRODUCTION

REPETITIVE control (RC) schemes are particularly suitable to achieve robust tracking of a periodic reference signal, see [1], [12], [18], [20]. Tracking of periodic signals is a common control problem in many relevant application fields, for example, in healthcare. In this article, the proposed analysis and controller design are motivated by the application of mechanical ventilation of patients on intensive care units (ICUs). Mechanical ventilation is used to support the breathing

of patients by providing the correct oxygen support and elimination of carbon dioxide [40]. In ventilation, tracking of a periodic signal, i.e., pressure target, is desired.

Several studies in the literature have focused on achieving accurate tracking performance for mechanical ventilation, e.g., [7], [17], [31], [34]. In particular, promising is the application of discrete-time–frequency domain RC in [32] and [29]. In this work, a significant reduction of the pressure tracking error is achieved. However, this is achieved under a linearity assumption of the considered ventilation system dynamics, whereas a mechanical ventilation system contains nonlinear system dynamics, see [30].

The considered ventilation system is a nonlinear dynamical system, which can be modeled as a Lur'e-type system. Lur'e-type systems consist of the interconnection of linear time-invariant dynamics with a static nonlinearity in the feedback loop. These systems form a practically relevant subclass of nonlinear systems, also for other application domains. To achieve robust tracking of the periodic pressure target of the ventilation system, a generically applicable RC scheme for Lur'e-type systems is developed.

The structural idea of RC is based on the *internal model principle*, namely, on the fact that when a periodic signal with known period T must be tracked, a copy of the disturbance model generating such a signal must be included in the regulator [5]. This is generally done through a universal generator of a T-periodic signal. Such a generator is implemented using a memory loop with a delay of length T. This memory loop places an infinite number of poles on the imaginary axes at the fundamental frequency $2\pi/T$ and its multiples, see [14], [12]. Then, the extended system composed by the plant and such memory loop is stabilized with feedback control.

Because a delay is easily implemented in discrete time, significant research efforts have been devoted to the development of discrete-time implementations of RC. In this approach, mostly linear systems are addressed from the theoretical point of view, and good tracking performance is achieved in these systems, see [6], [10], [21], [32], [35], [36]. Unfortunately, the developed frequency analysis tools cannot be directly employed in the presence of nonlinearities. Therefore, typically, no formal stability proofs are provided for RC applied to nonlinear systems.

In the existing literature, several studies have considered output tracking problems for continuous-time nonlinear systems. For instance, in [1], [8], [19], and [3], the problem of

output tracking for nonlinear systems that can be written in the canonical normal form is considered. In [22], incremental passivity concepts are used for the design of global regulators, and in [25], output regulation of Lur'e-type systems using convergent system properties is considered. However, a constructive design of the stabilizer and guaranteed harmonic regulation properties are not presented. The design in [2], [12], and [3] relies on state-feedback approaches, and the domain of attraction of the periodic solution is only local in the size of [2] and [3] or not discussed [12]. In [13], contractive feedback laws in tracking problems are developed for constant references, but not for periodic references. Finally, in [38], [39], and [37], a learning control approach has been developed to achieve tracking in nonlinear systems with repetitive disturbances. These methods show a significant improvement in tracking performance. In the scope of the challenge taken on in this article, a drawback of the work in [37], [39], and [38] is that these algorithms do not apply straightforwardly to Lur'e-type systems with (uncertain) output nonlinearities.

Although significant progress on output regulation for non-linear systems has been made, an intuitive RC scheme for nonlinear Lur'e-type systems with a formal stability guarantee is not yet available. To achieve this, a finite-dimensional realization of the exact RC scheme in [9] and [1] is used. The reason to consider a finite-dimensional realization is the difficulty to analyze the interconnection of an infinite-dimensional system, i.e., the internal model, with nonlinear plant dynamics with nonlinear outputs. In this article, we follow an approach that relies on the harmonic representation of the delay, see [2], [3], [12], [20]. The RC scheme is implemented by including a finite number n_o of linear oscillators in the control loop. This results in n_o poles on the imaginary axes at the frequency of the periodic reference and its multiples. Therewith, if the resulting closed-loop trajectories converge to a periodic solution, *harmonic regulation* of the tracking error is guaranteed. More precisely, the Fourier coefficients of the error signal corresponding to the frequencies embedded in the linear oscillators are zero, and the L^2-norm of the error signal is sufficiently small if n_o is large enough [2], [3], [12]. To guarantee the existence of globally asymptotically stable periodic solutions, the theory of convergent systems is exploited, see [23], [24], [26], [27]. To this end, we suppose that the static nonlinearity in the Lur'e-type system satisfies an incremental sector bound condition. Then, using the strictly positive real (SPR) lemma, sufficient conditions for a stabilizing output-feedback law are established. From a practical point of view, such an approach is interesting, because the conditions can be checked by visual inspection of the Nyquist plot and linear analysis tools (potentially using measured data only).

Eventually, this proposed repetitive controller design is applied to the practical problem of mechanical ventilation. The existing literature, e.g., [29], [32], has shown that frequency-domain RC can significantly improve the tracking performance in ventilation systems. However, because these ventilation systems are nonlinear, formal stability guarantees for the closed-loop system with RC are missing. Therefore, the control approach developed in this article is applied to this Lur'e-type ventilation system to improve its performance with formal stability guarantees.

Summarizing, the main contributions of this article are as follows:

1) the development of an RC strategy for nonlinear Lur'e-type systems, including a formal stability analysis;
2) the implementation and analysis of this RC scheme on the practical use case of a nonlinear mechanical ventilator, including experimental validation.

This article is organized as follows. In Section II, the problem statement is formalized. In Section III, the main results concerning the RC controller design are presented. Then, in Section IV, the RC paradigm is applied to the mechanical ventilation use case. Finally, the main conclusions and recommendations for future work are presented in Section V.

Notations: Throughout this article, s represents the Laplace variable. Given an $n \times n$ symmetric matrix P, we write $P \succ 0$ ($\prec 0$) if P is strictly positive (negative) definite. Given an $n \times n$ matrix P, the operator $\mathrm{blkdiag}(P \cdots P)$ represents a block-diagonal matrix with P as block-diagonal elements, and the dimensions are specified case-wise. Furthermore, $\dot{x}$ represents the continuous-time derivative of x. Finally, we define $\mathcal{P}_T(\tilde{r})$ as the set of C^1 T-periodic functions with bounded infinity norm and bounded infinity norm of its derivative. In particular, we say that $r(t) \in \mathcal{P}_T(\tilde{r})$ if r is C^1, T-periodic, and satisfies $\sup_{t \in [0,T]} |r(t)| \leq \tilde{r}$ and $\sup_{t \in [0,T]} |\dot{r}(t)| \leq \tilde{r}$ for some nonnegative real number $\tilde{r}$.

II. PROBLEM STATEMENT

In Section I, a gap in the existing literature has been identified in the application of RC to mechanical ventilation systems. More specifically, the commonly used frequency-domain RC does not provide formal stability guarantees when it is applied to Lur'e-type nonlinear ventilation systems. Therefore, in this section, a formal problem statement is formulated to develop RC for Lur'e-type systems.

Consider a single-input single-output (SISO) Lur'e-type system of the form

$$
\begin{aligned}
\dot{x} &= Ax + Bu + Ew \\
y &= Mx + Nw \\
w &= -\varphi(y) \\
v &= Cx + Dw
\end{aligned}
\tag{1}
$$

where $x \in \mathbb{R}^n$ is the state, $u \in \mathbb{R}$ is the control input, w and y are in $\mathbb{R}$, $v \in \mathbb{R}$ is the measured output, and $A, B, E, M, N, C,$ and D are real matrices of appropriate dimensions. The static nonlinearity $\varphi : \mathbb{R} \mapsto \mathbb{R}$ satisfies $\varphi(0) = 0$, and the following incremental sector bound condition:

$$
\underline{\varphi} \leq \frac{\varphi(y_1) - \varphi(y_2)}{y_1 - y_2} \leq \bar{\varphi} \quad \forall \, y_1 \neq y_2
\tag{2}
$$

for some known nonnegative constants $0 \leq \underline{\varphi} \leq \bar{\varphi}$. The control objective is to regulate the output v of (1) to a T-periodic

bounded reference $r \in \mathcal{P}_T(\tilde{r})$. Hence, the output regulation error is defined as follows:

$$e(t) := r(t) - v(t). \tag{3}$$

With the mechanical ventilation application in mind, where the full-state x is not available for feedback, we aim to design a dynamic output feedback controller for (1), processing only the regulated output error e, such that *harmonic regulation* is achieved in the following sense.

Problem 1 (Harmonic Regulation of Order n_o): Consider (1) with regulation error (3), and assume that the nonlinearity φ satisfies the incremental sector bound condition (2). Given any $\tilde{r} > 0$, $n_o > 0$, determine a dynamic output feedback controller of the form

$$\begin{aligned} \dot{z} &= \xi(z, e) \\ u &= \zeta(z, e) \end{aligned} \tag{4}$$

such that for any reference $r \in \mathcal{P}_T(\tilde{r})$ and any initial condition $x_{\mathrm{cl}}(0) := [x^T(0), z^T(0)]^T \in \mathbb{R}^{n_x}$, the corresponding steady-state trajectory $\bar{x}_{\mathrm{cl}} := [\bar{x}^T, \bar{z}^T]^T$ of the closed loop (1), (3), and (4) is bounded, T-periodic, and exponentially stable,[1] and the steady-state output error $\bar{e}$ has no harmonic content at frequencies $\omega = k 2\pi/T$, $k = 0, 1, \ldots, n_o$.

The RC approach in [2], [3], and [12] is followed to achieve the harmonic regulation objective stated in Problem 1. The main idea is to include linear oscillators at the periodic reference frequency and its multiples in the regulator dynamics (4). This approach achieves, if the closed-loop steady-state trajectories are bounded and periodic, structural zeros at the frequencies $k\omega$ with the blocking property of zeroing the Fourier coefficients of the output e corresponding to these frequencies. As a consequence, the strategy that we propose in this work is to do the following.

1) Design the function ξ in (4) to include the linear oscillators.
2) Design the feedback ζ in (4) to ensure the desired stability properties for the resulting closed-loop system.
3) Analyze the resulting trajectories, and show that the harmonic content is zero at the desired frequencies. As a byproduct, we verify that if the number of oscillators included in the regulator are large enough, the asymptotic ℓ^2-norm of the output e can be regulated to an arbitrarily small value.

III. RC OF LUR'E-TYPE SYSTEMS

In this section, the repetitive controller design for Lur'e-type systems is presented. First, in Section III-A, the repetitive controller design is presented, the closed-loop dynamics are obtained, and a loop transformation is applied that allows the use of known results on exponentially convergent Lur'e-type systems. In Section III-B, known results on convergent Lur'e-type systems are presented as a stepping stone to the stability analysis. Finally, in Section III-C, it is shown that the proposed controller design solves Problem 1.

[1] A time-varying solution $\bar{x}(t)$ is called exponentially stable if $\|x(x(0), t) - \bar{x}(\bar{x}(0), t)\| \le \alpha \|x(0) - \bar{x}(0)\| e^{-\lambda t}$ for some $\alpha, \lambda > 0$.

A. Controller Design

To provide a solution to Problem 1, the RC approach in [12] is adopted by including n_o linear oscillators in the control loop, at the reference frequency and its multiples, that process the output e to be regulated, as in standard output regulation problems, see [2], [3], [27]. To this end, the control structure in (4) is defined as follows:

$$\dot{z} = \xi(z, e) := \Phi z + \Gamma e \tag{5}$$
$$u = \zeta(z, e) := K z \tag{6}$$

where $z = \begin{bmatrix} z_0 \ z_1^T \ \cdots \ z_{n_o}^T \end{bmatrix}^T \in \mathbb{R}^{(2n_o+1)\times 1}$ with $z_0 \in \mathbb{R}$ and $z_k \in \mathbb{R}^{2\times 1}$ for $k = 1, \ldots, n_o$, and where the matrices $\Phi \in \mathbb{R}^{(2n_o+1)\times(2n_o+1)}$, $\Gamma \in \mathbb{R}^{(2n_o+1)\times 1}$, and $K \in \mathbb{R}^{1\times(2n_o+1)}$ are defined as follows:

$$\begin{aligned} \Phi &:= \mathrm{blkdiag}\big(0 \ \phi_1 \ \cdots \ \phi_{n_o}\big) \\ \Gamma &:= \begin{bmatrix} \gamma_0 \ \gamma_1^T \ \cdots \ \gamma_{n_o}^T \end{bmatrix}^T \\ K &:= \begin{bmatrix} \kappa_0 \ \kappa_1 \ \cdots \ \kappa_{n_o} \end{bmatrix} \end{aligned} \tag{7}$$

where

$$\phi_k := k \begin{bmatrix} 0 & \dfrac{2\pi}{T} \\ -\dfrac{2\pi}{T} & 0 \end{bmatrix}, \quad k = 1, \ldots, n_o \tag{8}$$

with $\gamma_0 \ne 0$ the integrator gain, such that z_0 embeds an integrator, and the matrix $\gamma_k \in \mathbb{R}^{2\times 1}$ is chosen, such that the pair (ϕ_k, γ_k) is controllable for any $k = 1, \ldots, n_o$. By construction, the pair (Φ, Γ) is, therefore, controllable. In this control structure, the z dynamics represent the state-space representation of n_o linear oscillators at the periodic reference frequency and its multiples. The number of oscillators n_o represents a degree of freedom of the controller design, as it defines the dimension of the chosen internal model, and allows to suppress the first n_o harmonics of the steady-state trajectory, which is formalized later.

Next, the closed-loop system consisting of the plant (1) and (3) and the repetitive controller (5) and (6) is written as a Lur'e-type system

$$\begin{aligned} \dot{x}_{\mathrm{cl}} &= A_{\mathrm{cl}} x_{\mathrm{cl}} + E_{\mathrm{cl}} w_{\mathrm{cl}} + d(t) \\ y_{\mathrm{cl}} &= M_{\mathrm{cl}} x_{\mathrm{cl}} + N_{\mathrm{cl}} w_{\mathrm{cl}} \\ w_{\mathrm{cl}} &= -\varphi(y_{\mathrm{cl}}) \end{aligned} \tag{9}$$

where

$$\begin{aligned} A_{\mathrm{cl}} &:= \begin{bmatrix} A & BK \\ -\Gamma C & \Phi \end{bmatrix}, \ E_{\mathrm{cl}} := \begin{bmatrix} E \\ -\Gamma D \end{bmatrix}, \ Q_{\mathrm{cl}} := \begin{bmatrix} 0 \\ \Gamma \end{bmatrix} \\ M_{\mathrm{cl}} &:= \begin{bmatrix} M \ 0 \end{bmatrix}, \quad N_{\mathrm{cl}} := N \end{aligned} \tag{10}$$

where $x_{\mathrm{cl}} := [x^T, z^T]^T \in \mathbb{R}^{n_x}$, $w_{\mathrm{cl}} := w$, $y_{\mathrm{cl}} := y$, and $d(t) := Q_{\mathrm{cl}} r(t)$, is a periodic, with period time T, time-varying piecewise continuous disturbance (induced by the periodic reference).

Next, a loop transformation as described in [16, Chapter 7] is applied to the closed-loop dynamics. This loop transformation gives an equivalent Lur'e-type system where the transformed nonlinearity $\tilde{\varphi}(y_{\mathrm{lt}})$ satisfies the incremental sector bound in (2) with $\underline{\tilde{\varphi}} = 0$ and $\overline{\tilde{\varphi}} = \infty$. This enables direct

application of the known results on exponentially convergent Lur'e-type systems in Section III-B. This loop transformation gives the following loop-transformed Lur'e-type system:

$$\dot{x}_{lt} = A_{lt}x_{lt} + E_{lt}w_{lt} + d(t)$$
$$y_{lt} = M_{lt}x_{lt} + N_{lt}w_{lt}$$
$$w_{lt} = -\tilde{\varphi}(y_{lt}) \tag{11}$$

where

$$A_{lt} := A_{cl} - \left(E_{cl}\underline{\varphi}\left(M_{cl} + N_{cl}\left(1 + \underline{\varphi}N_{cl}\right)^{-1}\underline{\varphi}M_{cl}\right)\right)$$
$$E_{lt} := E_{cl}\left(1 - \underline{\varphi}D_{cl}\left(1 + \underline{\varphi}N_{cl}\right)^{-1}\right)$$
$$M_{lt} := \phi M_{cl} - \phi N_{cl}\left(1 + \underline{\varphi}N_{cl}\right)^{-1}\underline{\varphi}M_{cl}$$
$$N_{lt} := 1 + \phi N_{cl}\left(1 + \underline{\varphi}N_{cl}\right)^{-1} \tag{12}$$

where $x_{lt} \in \mathbb{R}^{n_x}$, $y_{lt} \in \mathbb{R}$, $w_{lt} \in \mathbb{R}$, $\phi = \bar{\varphi} - \underline{\varphi}$, and $\tilde{\varphi}(y_{lt})$ satisfies the incremental sector bound in (2) with $\underline{\tilde{\varphi}} = 0$ and $\bar{\tilde{\varphi}} = \infty$. Furthermore, it is assumed that the controller is designed, such that Assumption 1 holds.

Assumption 1: The pair (A_{lt}, E_{lt}) is controllable, and the pair (A_{lt}, M_{lt}) in (11) is observable.

Next, to solve Problem 1, it must be shown that the closed-loop system exhibits a globally exponentially stable steady-state trajectory that is well defined, bounded, T-periodic, and that the associated output error $\bar{e}$ has no harmonic content at the frequencies included in the internal model. To show this, known results on exponentially convergent Lur'e-type systems are used. These results are provided next.

B. Exponentially Convergent Lur'e-Type Systems

First, we provide the following definition of convergent systems, see [23], [24], [33], applicable to the Lur'e-type systems of the form (11), with $\mathcal{D}$ a set of piecewise continuous, bounded disturbances.

Definition 1: Given $d(t) \in \mathcal{D}$, (11) is said to be globally exponentially convergent if the following hold.

1) There exists a solution $\bar{x}_{lt,d}(t)$ defined and bounded for all $t \in \mathbb{R}$.
2) The solution $\bar{x}_{lt,d}(t)$ is globally exponentially stable.

System (11) is called convergent for $d \in \mathcal{D}$ if it is convergent for any $d(t) \in \mathcal{D}$, see [27, Definition 2.16]. Note that for an exponentially convergent system, the steady-state solution is unique, see [27, Property 2.15]. Moreover, if the input $d(t)$ is T-periodic, then, for exponentially convergent systems, $\bar{x}_{lt,d}(t)$ is also T-periodic, as recalled in the next property, see [23], [24], [27].

Property 1: Consider (11), and suppose it is exponentially convergent. If d is a periodic signal with period $T > 0$, i.e., $d(t) = d(t + T)$ for all t, then the corresponding steady-state solution $\bar{x}_{lt,d}(t)$ is also periodic with period T.

To show that the closed-loop Lur'e-type system of the form (11) is a globally exponentially convergent system, let

$$\mathcal{H}(s) = M_{lt}(sI - A_{lt})^{-1}E_{lt} + N_{lt}. \tag{13}$$

Then, results from [41] and [27, Chapter 5] can be used. By combining the definition of an SPR transfer function and the incremental sector bound condition (2), Lemma 1 is obtained that expresses sufficient conditions that guarantee that (11) is globally exponentially convergent, which is proven in [16, Chapter 7].

Lemma 1: Let Assumption 1 hold. If (2) holds and the transfer function $\mathcal{H}(s)$ is SPR, then (11) is globally exponentially convergent.

Using Lemma 1, global exponential convergence of the closed-loop Lur'e-type system in (11) can be guaranteed by showing that $\mathcal{H}(s)$ is SPR. The transfer function $\mathcal{H}(s)$ is SPR if and only if the following conditions hold, see [23], [41].

1) $\mathcal{H}(s)$ is Hurwitz.
2) $\text{Re}\{\mathcal{H}(j\omega)\} > 0 \ \forall \omega \in \mathbb{R}$.
3) $\mathcal{H}(\infty) > 0$ or $\mathcal{H}(\infty) = 0$ and $\lim_{\omega\to\infty}\omega^2\mathcal{H}(j\omega) > 0$.

Note that the SPR conditions on $\mathcal{H}(s)$ can be visually verified with the Nyquist plot, see [16, Chapter 7]. This makes these conditions particularly useful to verify in practical applications, see Section IV. Next, these results are used to design the feedback gain K in the feedback law (6), such that Problem 1 is solved.

C. Harmonic Regulation of Lur'e-Type Systems

The results of Lemma 1 enable the main theoretical result of this article, which solves Problem 1. More specifically, it is shown that the presented repetitive controller achieves the desired harmonic regulation properties and convergence properties of the closed-loop system if the feedback gain K is designed properly.

If we can design the feedback law (6), such that the closed loop (1), (3), (5), and (6) is globally exponentially convergent for any $d(t)$, then by virtue of Definition 1 and Property 1, for every initial condition, the solutions of (9) exponentially converge to a unique, bounded, and well-defined steady-state solution, which is T-periodic if the reference $r(t)$ is T-periodic. Then, using Lemma 2 [2], [12], it is shown that the Fourier coefficients, of the associated steady-state solution $\bar{e}$ of the error e, corresponding to the n_o frequencies embedded in the internal model (5), must be zero. Hence, harmonic regulation is achieved.

Lemma 2: Let the steady-state solution $(\bar{x}, \bar{z})$ be a bounded trajectory of the cascade (1), (3), and (5), with the corresponding steady-state output error $\bar{e}(t)$. Suppose that $\bar{e}(t+T) = \bar{e}(t)$ for all $t \geq 0$. Then, necessarily

$$\int_0^T \cos\left(k\tfrac{2\pi}{T}t\right)\bar{e}(t)dt = \int_0^T \sin\left(k\tfrac{2\pi}{T}t\right)\bar{e}(t)dt = 0 \tag{14}$$

for all $k \in [0, 1, \ldots, n_o]$. Moreover, for any compact set $C_x \subset \mathbb{R}^n$, for any $\tilde{r} > 0$, $\bar{u} > 0$, and $\varepsilon > 0$, such that $\bar{x}(t) \in C_x$, $r \in \mathcal{P}_T(\tilde{r})$, and $|\bar{u}(t)| \leq \bar{u}$ for all $t \geq 0$, there exists $n_o^* \geq 1$, such that the following holds:

$$\|\bar{e}(t)\|_{L^2} := \left(\int_0^T |\bar{e}(t)|^2 dt\right)^{\frac{1}{2}} \leq \varepsilon \quad \forall\, n_o \geq n_o^*. \tag{15}$$

Note that a bound for ε can be computed following the proof of [2, Proposition 3]. This bound depends on the Lipschitz constant of the nonlinearity.

Then, combining these harmonic regulation properties and the convergent system properties of the loop-transformed closed-loop system solves Problem 1, which brings us to the result in Theorem 1.

Theorem 1: Consider the Lur'e-type system (1) and (3), with the nonlinearity $\varphi(\cdot)$ satisfying the incremental sector condition in (2), in closed loop with a dynamical controller (5) and (6). Given an arbitrary integer $n_o > 0$ and suppose that the matrix K is chosen, such that the transfer function $\mathcal{H}(s)$ in Lemma 1, with the matrices A_{lt}, E_{lt}, M_{lt}, and N_{lt} defined in (10), satisfies Assumption 1 and the SPR conditions in Lemma 1. Then, Problem 1 is solved, namely, harmonic regulation of order n_o, as defined by (14), is achieved.

Proof: Consider (1) and (3) in closed loop with (5) and (6), which can be written in the form of (9) and (10). Then, the loop transformation can be applied to obtain (11) and (12). Since the conditions of Lemma 1 are satisfied and the loop-transformed system is equivalent to the original closed-loop system, the closed-loop system is globally exponentially convergent. Hence, by Property 1, if $r(t)$ is periodic with period $T > 0$, there exists a bounded, globally exponentially stable solution $\bar{x}(t)$ and $\bar{z}(t)$, which is T-periodic. As a consequence, the resulting output steady-state trajectory $\bar{e}$ is also bounded and T-periodic. By direct application of Lemma 2, it satisfies (14). This concludes the proof. $\square$

The statement of Theorem 1 establishes a set of sufficient conditions for the design of the regulator in (5) and (6). In particular, the matrices K and Γ should be designed, such that the desired SPR conditions on $\mathcal{H}(s)$ are satisfied to ensure the satisfaction of the conditions in Lemma 1. The SPR conditions at the end of Section III-B can be supported by graphical checks in a Nyquist plot, similar to frequency-domain design techniques for linear controller design.

In case the system in (9) is a minimum-phase system with unitary relative degree,[2] a systematic design of the gain K can be done by the following [3]. The system in (9) can be put in this form, for instance, when $CB \neq 0$ and $D = 0$. In such case, it can be put in the canonical normal form following [15, Chapter 4]. Then, additional properties can be established. In particular, by selecting K, such that the bound

$$K\Gamma\Gamma^T K^T \leq a \qquad (16)$$

holds with a a positive and bounded scalar, which is independent of n_o, it can be proved that the asymptotic L^2-norm of $\bar{e}$ can be made arbitrarily small by increasing the number of oscillators. More specifically, in such case, ϵ in (15) can be made arbitrarily small by increasing the number of oscillators n_o. For instance, one can match condition (16) by selecting the gains γ_k in (7) as $\gamma_k = k^{-(1+\epsilon)}\bar{\gamma}_k$ with $\bar{\gamma}_k$, so that $|\bar{\gamma}_k| \leq \bar{\gamma}$ for any $k = 1, \ldots, n_o$, for some $\bar{\gamma} > 0$, and by selecting κ_k in (7), such that $|\kappa_k| \leq \bar{\kappa}$ for any $k = 1, \ldots, n_o$, for some $\bar{\kappa} > 0$. Note that condition (16) essentially establishes that the regulator (5) and (6) has an L^2 gain between the input e and the output u, which does not depend on the number of

[2] In this case, we refer to a system in normal form with stable zero dynamics. See, for instance, (2) and [1, Assumption 2]. Necessary and sufficient conditions under which a system of the form (9) can be written in canonical normal form are well known in the literature, see [15].
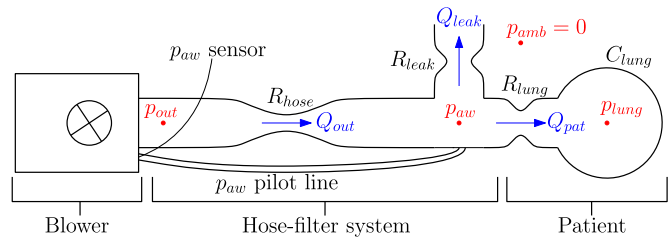

Fig. 1. Schematic of the blower-hose-patient system, with the corresponding resistances, lung compliance, pressures, and flows.

oscillators n_o. The complete proof of this property is given in [3, Lemma 3]. Intuitively, the main idea behind such a choice is to put decreasing weights on higher harmonics in order to obtain a bounded gain when summing up the contribution of the L^2 gain of all oscillators.

This design philosophy will be pursued in the mechanical ventilation application to experimentally show the desired approximate L^2 output regulation objective (15).

IV. APPLICATION TO MECHANICAL VENTILATION

In this section, the RC strategy is applied to a nonlinear mechanical ventilation system; i.e., this section describes the second contribution of this article. First, in Section IV-A, an overview of the considered ventilation system and the control goal for ventilation are described. Thereafter, the mathematical ventilation model and the actual mechanical ventilation setup are presented in Section IV-B. Then, repetitive controllers for mechanical ventilation are designed, and stability of the closed-loop system is analyzed in Section IV-C. Then, in Section IV-D, the experimental results are presented and analyzed. Thereafter, another ventilation use case is briefly considered to analyze the conservatism of Theorem 1 in Section IV-E. Finally, a remark on RC design is made based on observations from the experimental case study.

A. Ventilation System Overview and Control Goal

Mechanical ventilators are essential equipment in ICUs to assist patients who cannot breathe on their own or need support to breathe sufficiently. The goal of mechanical ventilation is to ensure adequate oxygenation and carbon dioxide elimination [40], thereby sustaining the patient's life. Next, the considered ventilation system and corresponding control goal are described.

1) Ventilation System Overview: A schematic overview of the considered ventilation system is depicted in Fig. 1. The main components of this system are the blower, the hose-filter system, and the patient. A centrifugal blower compresses ambient air to achieve the desired blower outlet pressure p_{out}. The difference between p_{out} and the airway pressure p_{aw} results in the outlet flow Q_{out} through the hose. This hose is modeled using a nonlinear hose model. The flow through the hose, i.e., the outlet flow Q_{out}, is divided into a patient flow Q_{pat} and a leak flow Q_{leak}. The intended leak near the patient is used to flush CO_2-rich air from the system. Finally, the patient's lungs are inflated and deflated by the patient flow.
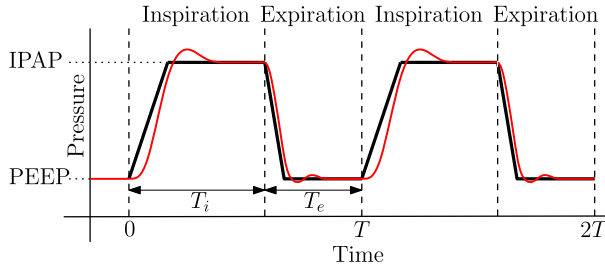
This article has been accepted for inclusion in a future issue of this journal. Content is final as presented, with the exception of pagination.

6

IEEE TRANSACTIONS ON CONTROL SYSTEMS TECHNOLOGY

Fig. 2.   Typical airway pressure for two breathing cycles of PCV, showing the set point (——) and the typical response (——).
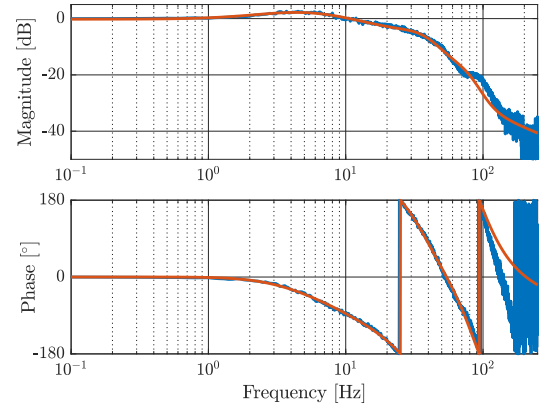

Fig. 3.   FRF (——) and the sixth-order identified parametric model (——) of the blower, i.e., from p_c to p_{out}.
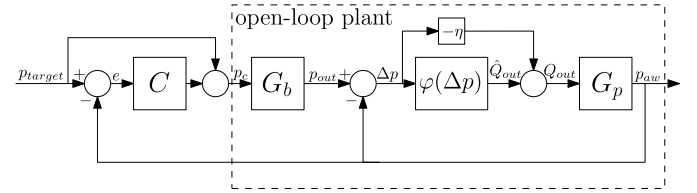

Fig. 4.   Block diagram of the full ventilation system, with G_b the blower dynamics, C an arbitrary feedback controller, G_p the patient-leak dynamics, and $\varphi(\Delta p) = R_{hose}(\Delta p) + \eta \Delta p$ the nonlinear hose model.

2) Control Goal: In this experimental use case, pressure controlled ventilation (PCV) is considered. A schematic example of PCV is depicted in Fig. 2. In PCV, the pressure near the patient's mouth, the airway pressure p_{aw}, should track a desired pressure target p_{target}, i.e., $r := p_{target}$. On a preset periodic interval, of length T, the pressure level is increased to the inspiratory positive airway pressure (IPAP) and consequently lowered to the positive end-expiratory pressure (PEEP). These varying pressure levels ensure the desired airflow in and out of the patient's lungs. The total breath length T consists of the inspiration time T_i and expiration time T_e, i.e., $T = T_i + T_e$.

The control goal for PCV is to achieve a small tracking error $e := r - p_{aw} = r - v$, where the reference $r(t)$ is a time-varying signal that is perfectly periodic with an interval length T, i.e., $r(t) = r(t + T)$ for a known $T > 0$ and all $t \geq 0$. Because of this periodicity property and the nonlinear nature of the hose model, the RC strategy developed in this article is particularly suitable for this application.

B. Mathematical Model and Experimental Ventilation System

For controller design and the stability analysis, a mathematical Lur'e-type system model is derived. The ventilation model is based on [30]. Thereafter, the actual experimental ventilation setup is presented.

1) Mathematical Model of the Ventilation System: In this section, first, the separate models for the plant components are derived, i.e., blower model G_b, hose model R_{hose}, and patient-leak model G_p. Thereafter, these models are combined to obtain the open-loop Lur'e-type ventilation system model for the controller design and associated stability analysis. The complete plant and the considered control strategy are visualized in the block diagram in Fig. 4.

The blower model G_b is obtained by means of the sixth-order fit of a frequency response measurement (FRF) of the actual blower dynamics [28]. This state-space model accurately describes the input–output relation of the blower, i.e., from the control signal p_c to the blower output p_{out}. The measured FRF and the blower model G_b are depicted in Fig. 3, showing that G_b is an accurate representation of the FRF measurement of the actual blower. The blower G_b is modeled as the following state-space system:

$$\dot{x}_b = A_b x_b + B_b p_c$$
$$p_{out} = C_b x_b \qquad (17)$$

with $x_b \in \mathbb{R}^6$, $p_c \in \mathbb{R}$, $p_{out} \in \mathbb{R}$, and system matrices of appropriate dimensions.

The hose is modeled by the nonlinear hose resistance R_{hose}, as presented in [30], which describes the relation between the flow through the hose Q_{out} and the pressure drop over the hose $\Delta p := p_{out} - p_{aw}$. From experiments, it is concluded that the hose can be modeled as follows:

$$Q_{out} := R_{hose}(\Delta p)$$
$$= \text{sign}(\Delta p) \frac{-R_1 + \sqrt{R_1^2 + 4R_2|\Delta p|}}{2R_2} \qquad (18)$$

where R_1 and R_2 are the hose-resistance parameters.

Next, the combined patient-leak model G_p describes the relation between the outlet flow Q_{out} and the system output $y = p_{aw}$. This patient model is described by the following first-order state-space model, based on the linear one-compartmental lung model in [4]:

$$\dot{p}_{lung} = a_p p_{lung} + b_p Q_{out}$$
$$p_{aw} = c_p p_{lung} + d_p Q_{out} \qquad (19)$$

with

$$a_p = -\frac{1}{C_{lung}(R_{leak} + R_{lung})}$$

$$b_p = \frac{R_{leak}}{C_{lung}(R_{leak} + R_{lung})}$$

$$c_p = \frac{R_{leak}}{R_{leak} + R_{lung}}, \quad d_p = \frac{R_{leak}R_{lung}}{R_{leak} + R_{lung}}. \qquad (20)$$

Finally, these separate models are combined to obtain the open-loop plant model, as depicted inside the dashed box in

Fig. 4. Note that an additional term $\eta\Delta p$ is added to the nonlinear hose resistance, i.e., $\varphi(\Delta p) := R_{\text{hose}}(\Delta p) + \eta\Delta p$, and subtracted in the parallel path; this is included to ensure that the linear dynamics of the open-loop plant in Lur'e-type form are controllable and observable. The total system's dynamics, i.e., the full Lur'e-type ventilation system, are independent of the choice of $\eta \in \mathbb{R}$.

To obtain the open-loop plant model, the blower, hose, and patient model are combined. This gives the open-loop model from p_c to p_{aw} in the form of (1). The open-loop ventilation system is defined by (1) with the system matrices

$$
\begin{aligned}
A &= \begin{bmatrix} A_b & 0 \\ -(1-\eta d_p)^{-1}\eta C_b b_p & a_p + \eta c_p(1-\eta d_p)^{-1} b_p \end{bmatrix} \\
B &= \begin{bmatrix} B_b \\ 0 \end{bmatrix}, \quad E = \begin{bmatrix} 0 \\ -b_p(1-\eta d_p)^{-1} \end{bmatrix} \\
M &= \begin{bmatrix} C_b + d_p(1-\eta d_p)^{-1}\eta C_b \\ -c_p - d_p(1-\eta d_p)^{-1}\eta c_p \end{bmatrix}^T \\
N &= d_p(1-\eta d_p)^{-1}, \quad D_o = -d_p(1-\eta d_p)^{-1} \\
C &= \begin{bmatrix} -d_p(1-\eta d_p)^{-1}\eta C_b & c_p + d_p(1-\eta d_p)^{-1}\eta c_p \end{bmatrix}
\end{aligned} \quad (21)
$$

and the nonlinearity

$$
\varphi(y) := R_{\text{hose}}(y) + \eta y. \quad (22)
$$

These open-loop system matrices and the nonlinearity in combination with the RC that is designed in Section IV-C are used to retrieve the closed-loop ventilation system and to guarantee that it solves Problem 1 using Theorem 1.

2) Experimental Ventilation Setup: The main components of the experimental setup used in this case study are depicted in Fig. 5. The figure shows the Macawi blower-driven mechanical ventilation module [11]. The dSPACE system (dSPACE GmbH, Paderborn, Germany) is used to implement the controls in MATLAB Simulink (MathWorks, Natick, MA, USA). Furthermore, the ASL 5000[3] Breathing Simulator (IngMar Medical, Pittsburgh, PA, USA) represents the patient. This lung simulator can be used to emulate a wide variety of patients with a linear resistance and compliance. Furthermore, a typical ventilation hose with leak is used to attach the ventilation module to the lung simulator. The system parameters that are used for the stability analysis are shown in Table I. The leak and hose parameters are obtained by a calibration, and the patient parameters are the settings used on the mechanic lung simulator, i.e., patient emulator in Fig. 5.

The analysis in Section IV-C is done using a continuous-time representation of the controller and plant model. However, the controller is implemented in dSPACE using a discrete-time representation of the continuous-time control strategy. The discrete-time controllers are obtained using the zero-order hold discretization scheme at a sampling frequency of 500 Hz. This sampling frequency is significantly higher than the relevant system dynamics, e.g., the blower shows strong roll-off at frequencies above 10 Hz. Furthermore, 500 Hz is significantly higher that the frequency content of the reference signal. Therefore, the continuous-time controller
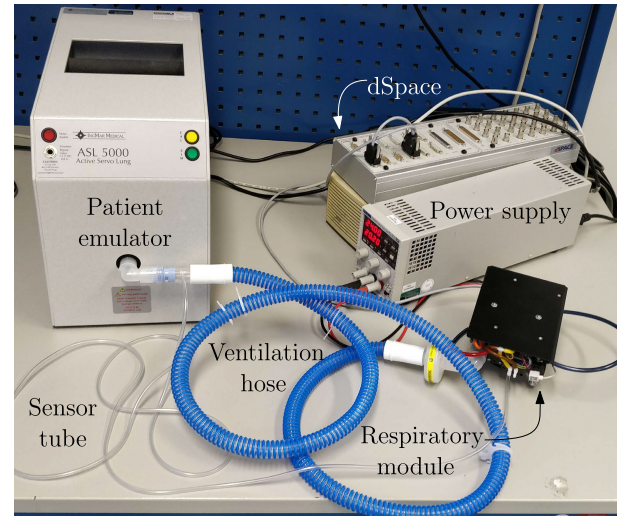
[3]Trademarked.

Fig. 5. Experimental setup with the mechanic patient simulator, the respiratory module, the ventilation hose, and the dSPACE module.

TABLE I
RELEVANT SYSTEM AND EXPERIMENT PARAMETER
FOR THE STABILITY ANALYSIS

Parameter	Value	Unit
R_{leak}	24	mbar s/L
R_1	2.8	mbar s/L
R_2	1.6	mbar s^2/L^2
R_{lung}	5	mbar s/L
C_{lung}	50	mL/mbar
η	-0.1	mL/s/mbar

design and stability analysis are deemed relevant for this application.

C. Controller Design for Mechanical Ventilation

Next, the RC controller design for mechanical ventilation is described, and it is shown that it solves Problem 1 for this ventilation use case.

1) Controller Design: For the design of the feedback controller C in Fig. 4, the control strategy in (5), (7), and (8) with feedback law (6) is followed. This means that the feedback controller C consists of an integrator and n_o oscillators from the first up until the n_o^{th} harmonic of the breathing frequency $\omega_b = 2\pi/T$ rad/s. Besides this feedback controller, a unity feedforward controller, as depicted in Fig. 4, is used. The unity feedforward term is included to improve the overall regulation accuracy. Note that it does not affect stability, since it is included in the closed-loop ventilation system through the disturbance term d in (9). The stability analysis is independent of this disturbance in view of the convergence properties of the closed-loop dynamics.

For the final RC design, different controllers are designed to analyze the effect of the number of oscillators, i.e., $n_o \in \{0, 1, 5, 15, 20\}$. We select the integrator gain as $\gamma_0 = 2\pi$ and oscillator gains as $\gamma_k = \begin{bmatrix} 1 & 1 \end{bmatrix}(2/k^{1+\epsilon})$ with $\epsilon = 0.4$, for $k = 1, 2, \ldots, n_o$. The feedback law is chosen as $K \in \mathbb{R}^{1 \times (2n_o+1)}$ with all entries 1. Note that the design of the gains Γ, K satisfies (16). Next, the stability properties of
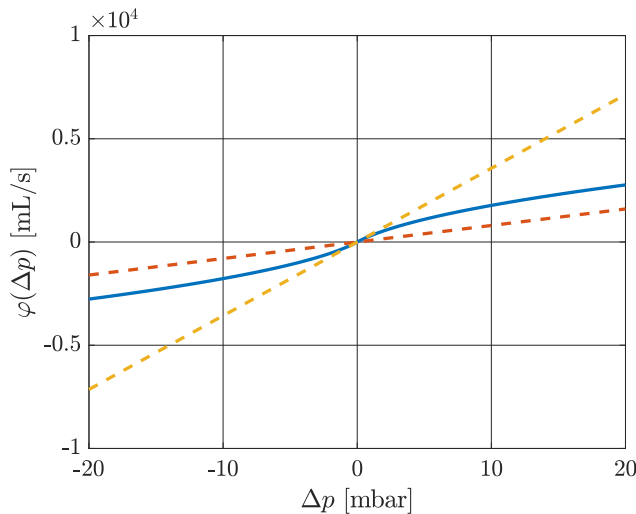
Fig. 6. Visualization of the nonlinearity $\varphi(\Delta p)$ (——), and its sector bounds $\underline{\varphi}\Delta p$ (- - -) and $\bar{\varphi}\Delta p$ (- - -), showing that the incremental sector condition holds for $[\underline{\varphi}, \bar{\varphi}] = [80, (1/R_1) + \eta]$.

Fig. 7. Nyquist plot of $\mathcal{H}(s)$ for $n_o = 0$ (——), $n_o = 1$ (——), $n_o = 5$ (——), $n_o = 15$ (——), and $n_o = 20$ (——). The figure shows that $\text{Re}(\mathcal{H}(j\omega)) > 0 \forall \omega \in [-\infty, \infty]$.

the closed-loop ventilation system with the RC controller are analyzed.

2) Stability Analysis: To guarantee exponential convergence of the closed-loop ventilation system, and therewith showing that Problem 1 is solved, Theorem 1 is verified. First of all, the controlled system is written in the closed-loop form of (9), and the upper $\bar{\varphi}$ and lower $\underline{\varphi}$ sector bounds of the nonlinearity $\varphi(y)$ in (22) are computed. Using these bounds, the loop transformation is applied to obtain the system in (11). Thereafter, Lemma 1 is verified, which ensures that Theorem 1 holds.

The upper sector bound $\bar{\varphi}$ is defined by taking the derivative of $\varphi(\Delta p)$ at the origin, where the slope of φ is the largest, see Fig. 6, which gives $\bar{\varphi} = (1/R_1) + \eta$. The lower sector bound $\underline{\varphi}$ is obtained from visual inspection, such that it holds on a finite domain of $\Delta p \in [-20, 20]$ mbar; this domain is sufficient for the practical application of ventilation. This leads to the sector $\varphi \in [\underline{\varphi}, \bar{\varphi}] = [80, (1/R_1) + \eta]$ for the nonlinearity in (22). The nonlinearity and these sector bounds are visualized in Fig. 6.

Using these sector bounds, the loop transformation is performed to obtain the system in (11), and it is verified that the pair $(A_{\text{lt}}, E_{\text{lt}})$ is controllable, and the pair $(A_{\text{lt}}, M_{\text{lt}})$ is observable for every n_o; i.e., Assumption 1 holds. Thereafter, $\mathcal{H}(s)$ is constructed using the matrices of the loop-transformed system.

Then, it is guaranteed that $\mathcal{H}(s)$ is SPR, and it is first verified that for all $n_o \in \{0, 1, 5, 15, 20\}$, the transfer function $\mathcal{H}(s)$ is Hurwitz, which is verified by computing the poles and checking that they reside in the open left half-plane. Thereafter, it is graphically validated that $\text{Re}(\mathcal{H}(j\omega)) > 0 \ \forall \omega \in [-\infty, \infty]$. This is validated in Fig. 7; it is clearly shown that for all considered values of n_o, the real part of $\mathcal{H}(j\omega)$ is strictly positive. Finally, it is verified that $\mathcal{H}(\infty) > 0$. This is also the case for all $n_o \in \{0, 1, 5, 15, 20\}$.

From these results, Lemma 1, and Theorem 1, it is concluded that the nonlinear closed-loop ventilation system is
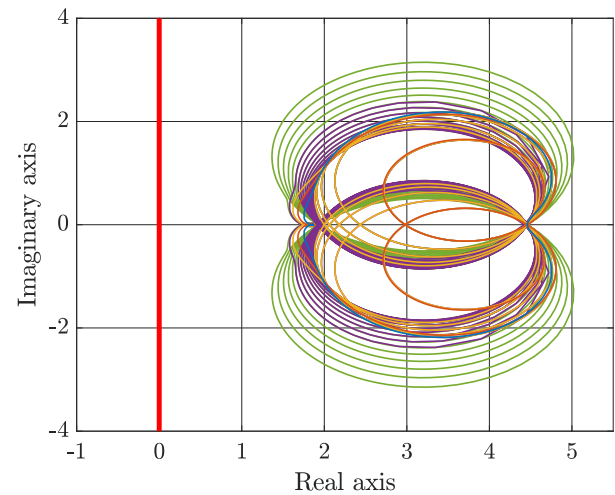
exponentially convergent on a compact domain[4] in state space for which $\Delta p \in [-20, 20]$ mbar, and that this controller solves the RC problem. Next, the performance of the different controllers is analyzed by means of experiments.

Remark 1: To ensure the stability of systems with slowly varying parameters (which is typically the case for this mechanical ventilation case), an approach similar to [32] could be followed. One could design a single controller for a nominal parametric setting and prove the stability property for a variety of (slowly, i.e., quasi-constant) varying parameters. This can be achieved by ensuring the SPR property for the linear dynamics of the Lur'e-type system for a set of parameters, e.g., lung compliances.

D. Experimental Results for Mechanical Ventilation

The main experimental results are shown in Figs. 8 and 9. The time-domain results of the 20th breath with the integrator only, i.e., $n_o = 0$, and the repetitive controller with 20 oscillators, i.e., $n_o = 20$, are visualized in Fig. 8. The top plot shows the reference and the measured outputs, and the bottom plot shows the tracking error for both controllers. The figure clearly shows that the tracking error is significantly reduced by the repetitive controller. The overshoot is eliminated, and the rise time is significantly shorter. Note that the residual error with RC contains oscillatory behavior, especially during the expiration at PEEP level, i.e., between 82 and 84 s. These oscillations contain mostly frequency content higher than 20 times the breathing frequency, i.e., above 5 Hz. It is observed that the tracking error's frequency content at frequency above the n_o^{th} harmonic is increased. In Section IV-F, a remark and analysis of this phenomenon are included, since this phenomenon could potentially deteriorate the system's tracking performance.

The ℓ^2-norm of the error per breath for every controller is shown in Fig. 9. The ℓ^2-norm of the error of a particular

[4]Such domain can be explicitly formulated using a quadratic Lyapunov function following from the Kalman–Yakubovich lemma for the SPR transfer function $\mathcal{H}(s)$.
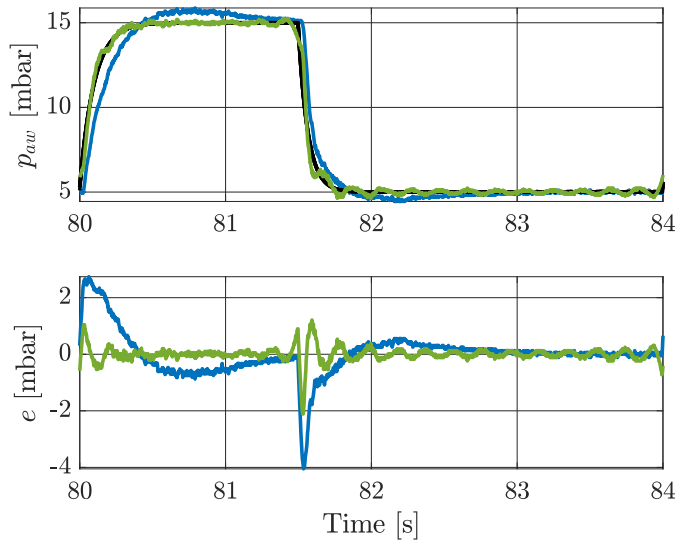
Fig. 8. Time domain results upon convergence for $n_o = 0$ (———) and $n_o = 20$ (———), and the target pressure (———). The figure shows that the error is significantly reduced by the repetitive controllers.
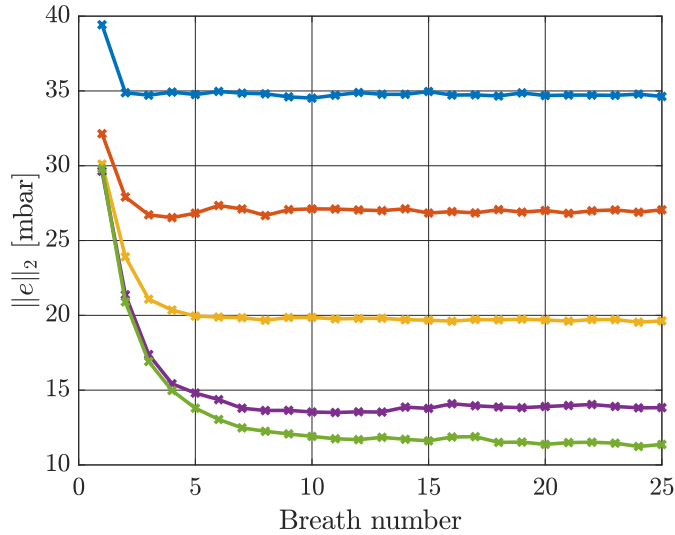

Fig. 9. ℓ^2-norm of the error for every breath for $n_o = 0$ (———), $n_o = 1$ (———), $n_o = 5$ (———), $n_o = 15$ (———), and $n_o = 20$ (———). The figure shows that more oscillators result in a smaller error, and the controllers converge in approximately ten breaths.

breath j is defined as $\|e\|_2 = (\sum_{k=1+(j-1)\rho}^{j\rho} |e(k)|^2)^{(1/2)}$ with $\rho = (T/\Delta T)$ and ΔT the sampling time. The figure clearly shows that increasing the number of oscillators reduces the ℓ^2-norm of the error upon convergence. Including 20 oscillators in the loop reduces the ℓ^2-norm of the error by more than a factor of 3 compared with integral action only. Furthermore, it is observed that the convergence time is longer for an increasing number of oscillators, and the controller with 20 oscillators converges in approximately 15 breaths.

Concluding, all controllers show convergent behavior in the experiments, as expected by the analysis. Furthermore, the tracking error is reduced significantly, by more than a factor of 3, by including RC. The Fourier coefficients of the steady-state output error $\bar{e}(t)$ are suppressed at the frequencies $w = k(2\pi/T)$, $k = 0, 1, \ldots, n_o$.
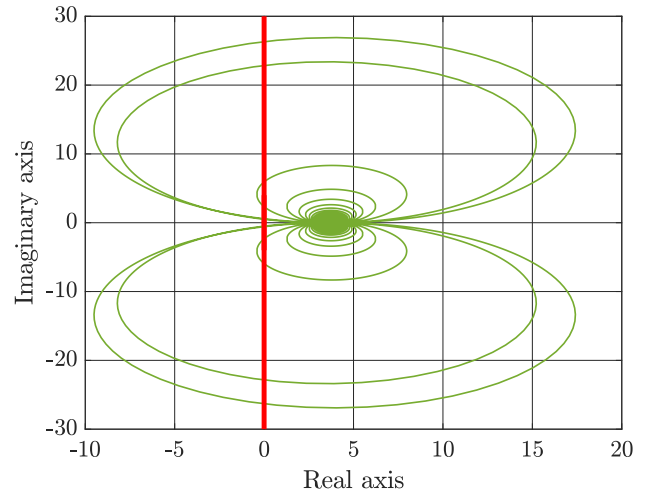

Fig. 10. Nyquist plot of $\mathcal{H}(s)$ for $n_o = 20$ (———) for the baby use case. The figure shows that $\text{Re}(\mathcal{H}(j\omega)) > 0 \forall \omega \in [-\infty, \infty]$ does not hold; hence, convergence is not guaranteed.

E. Analysis of Conservatism

To analyze how conservative the convergence properties of Theorem 1 are, an experimental use case is presented where the SPR properties are violated. This is achieved by considering a ventilation use case with lung parameters that represent a baby patient; i.e., $C_{\text{lung}} = 3$ mL/mbar and $R_{\text{lung}} = 50$ mbar s/L. The same hose and blower system as for the adult use case are used; hence, the same sector conditions for the linearity can be used. Furthermore, the same RC design as for the adult use case is followed for $n_o = 20$. The transfer function $\mathcal{H}(s)$ is computed for this system and visualized in Fig. 10. This figure clearly shows that the second condition for SPR transfer functions is violated for $n_o = 20$. Therefore, the desired convergence properties of the system cannot be guaranteed for this controller design with $n_o = 20$ oscillators.

The resulting ℓ^2-norm of the error per breath is shown in Fig. 11. This figure clearly shows that the system behaves unstable for $n_o = 20$. Concluding, this use case shows that the sufficient conditions in Theorem 1 have limited conservatism, which is a desirable property for practical controller design, because it allows more design freedom.

F. Remark on Repetitive Controller Design

In the experimental analysis, especially in the baby use case, it is observed that the remaining error consists of oscillations at frequencies above the harmonics of the n_o^{th} oscillator. These oscillations in the error are increasing for an increasing number of oscillators, limiting the overall tracking performance. Especially, in other use cases, it is observed that increasing the number of oscillators can significantly deteriorate the system performance. This effect can be explained by analyzing the sensitivity S_{re}, i.e., transfer function from the reference r to the tracking error e, of a linearization of the closed-loop ventilation system. This linearized closed-loop system is obtained by replacing the nonlinearity in Fig. 4 by a linear resistance; i.e., $R_{\text{hose}}(\Delta p)$ is replaced by $(\Delta p / R_{\text{lin}})$ with $R_{\text{lin}} = (2/\underline{\varphi} + \bar{\varphi})$, and $\eta = 0$. The resulting Bode magnitude plot of $\overline{S}_{\text{re}}$ is

This article has been accepted for inclusion in a future issue of this journal. Content is final as presented, with the exception of pagination.

10
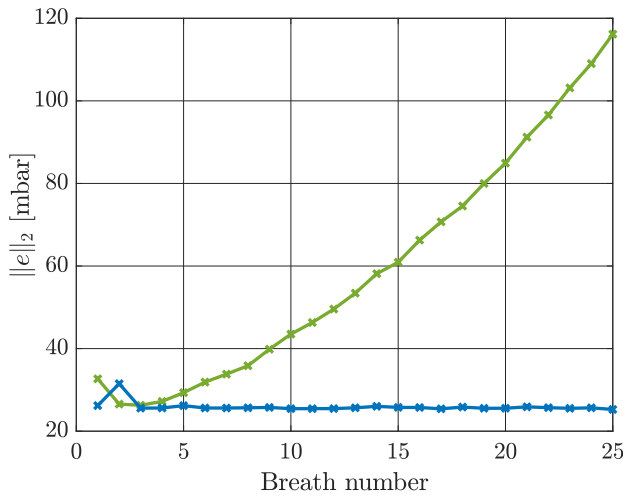
IEEE TRANSACTIONS ON CONTROL SYSTEMS TECHNOLOGY

Fig. 11. ℓ^2-norm of the error for every breath for $n_o = 0$ (———), and $n_o = 20$ (———) for the baby use case. The figure shows unstable behavior for that the closed-loop system with $n_o = 20$.
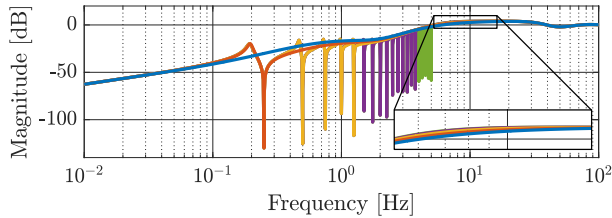

Fig. 12. Bode magnitude plot of the sensitivity S_{re} for the linearization of the closed-loop system with $n_o = 0$ (———), $n_o = 1$ (———), $n_o = 5$ (———), $n_o = 15$ (———), and $n_o = 20$ (———). The figure shows a magnitude increase at frequencies around 8 Hz, causing oscillations at these frequencies.

shown in Fig. 12. This Bode magnitude plot clearly shows that the tracking error is zero at the harmonics of the breathing frequencies. However, it also shows an increase in magnitude at frequency above the oscillator frequencies. The magnitude at these frequencies is increasing for an increasing number of oscillators. This increase in magnitude causes the oscillations at these frequencies as shown in the experiments. Therefore, in future work, it should be analyzed how this increase in magnitude at these specific frequencies can be eliminated.

V. CONCLUSION AND FUTURE WORK

In this article, an RC scheme that achieves robust tracking for nonlinear Lur'e-type systems with stability guarantees is presented. The RC scheme is composed of a dynamical system consisting of n_o linear oscillators at the reference's period and its multiples, which represents the internal model, processing the tracking error, and a pure integral controller guaranteeing the closed-loop system to be convergent. This convergence property ensures that the steady-state trajectory is periodic, and therefore, harmonic regulation is achieved at the frequencies included in the internal model.

This RC scheme is successfully implemented in a mechanical ventilation system for ICUs, a medical application to support the breathing of patients. Through a stability analysis based on the Nyquist plot, it is shown that this closed-loop ventilation system is convergent, and hence, the designed controller solves the RC problem at hand. In addition, it is

also shown experimentally that by increasing the number of oscillators, the asymptotic L^2-norm of the regulated output is reduced. Furthermore, experiments show that the presented controller design is able to significantly improve pressure tracking when compared with pure integral action.

REFERENCES

[1] D. Astolfi, S. Marx, and N. van de Wouw, "Repetitive control design based on forwarding for nonlinear minimum-phase systems," *Automatica*, vol. 129, Jul. 2021, Art. no. 109671.

[2] D. Astolfi, L. Praly, and L. Marconi, "Approximate regulation for nonlinear systems in presence of periodic disturbances," in *Proc. 54th IEEE Conf. Decis. Control (CDC)*, Osaka, Japan, Dec. 2015, pp. 7665–7670.

[3] D. Astolfi, L. Praly, and L. Marconi, "Nonlinear robust periodic output regulation of minimum phase systems," *Math. Control, Signals, Syst.*, vol. 34, no. 1, pp. 129–184, Mar. 2022.

[4] J. H. T. Bates, *Lung Mechanics*. Cambridge, U.K.: Cambridge Univ. Press, 2009.

[5] M. Bin, D. Astolfi, and L. Marconi, "About robustness of control systems embedding an internal model," *IEEE Trans. Autom. Control*, early access, Feb. 14, 2022, doi: 10.1109/TAC.2022.3151574.

[6] L. Blanken, S. Koekebakker, and T. Oomen, "Multivariable repetitive control: Decentralized designs with application to continuous media flow printing," *IEEE/ASME Trans. Mechatronics*, vol. 25, no. 1, pp. 294–304, Feb. 2020.

[7] M. Borrello, "Modeling and control of systems for critical care ventilation," in *Proc. Amer. Control Conf. (ACC)*, 2005, pp. 2166–2180.

[8] C. I. Byrnes and A. Isidori, "Nonlinear internal models for output regulation," *Trans. Autom. Control*, vol. 49, no. 12, pp. 2244–2247, Dec. 2004.

[9] F. Califano, M. Bin, A. Macchelli, and C. Melchiorri, "Stability analysis of nonlinear repetitive control schemes," *IEEE Control Syst. Lett.*, vol. 2, no. 4, pp. 773–778, Oct. 2018.

[10] R. Costa-Castelló and R. Griñó, "A repetitive controller for discrete-time passive systems," *Automatica*, vol. 42, no. 9, pp. 1605–1610, Sep. 2006.

[11] OEM Solutions. (2021). *DEMCON Macawi Respiratory Systems*. Accessed: May 3, 2019. [Online]. Available: https://www.macawi.com/products-services/

[12] J. Ghosh and B. Paden, "Nonlinear repetitive control," *IEEE Trans. Autom. Control*, vol. 45, no. 5, pp. 949–954, May 2000.

[13] M. Giaccagli, D. Astolfi, V. Andrieu, and L. Marconi, "Sufficient conditions for global integral action via incremental forwarding for input-affine nonlinear systems," *IEEE Trans. Autom. Control*, vol. 67, no. 12, pp. 6537–6551, Dec. 2022.

[14] S. Hara, Y. Yamamoto, T. Omata, and M. Nakano, "Repetitive control system: A new type servo system for periodic exogenous signals," *IEEE Trans. Autom. Control*, vol. AC-33, no. 7, pp. 659–668, Jul. 1988.

[15] A. Isidori, *Nonlinear Control Systems*. Berlin, Germany: Springer, 1995.

[16] H. K. Khalil, *Nonlinear Systems*, vol. 3. Upper Saddle River, NJ, USA: Prentice-Hall, 2002.

[17] H. Li and W. M. Haddad, "Model predictive control for a multi-compartment respiratory system," in *Proc. Amer. Control Conf. (ACC)*, Jun. 2012, pp. 5574–5579.

[18] R. W. Longman, "On the theory and design of linear repetitive control systems," *Eur. J. Control*, vol. 16, no. 5, pp. 447–496, Jan. 2010.

[19] L. Marconi, L. Praly, and A. Isidori, "Output stabilization via nonlinear Luenberger observers," *SIAM J. Control Optim.*, vol. 45, no. 6, pp. 2277–2298, Jan. 2007.

[20] P. Mattavelli and F. P. Marafao, "Repetitive-based control for selective harmonic compensation in active power filters," *IEEE Trans. Ind. Electron.*, vol. 51, no. 5, pp. 1018–1024, Oct. 2004.

[21] Y. Onuki and H. Ishioka, "Compensation for repeatable tracking errors in hard drives using discrete-time repetitive controllers," *IEEE/ASME Trans. Mechatronics*, vol. 6, no. 2, pp. 132–136, Jun. 2001.

[22] A. Pavlov and L. Marconi, "Incremental passivity and output regulation," *Syst. Control Lett.*, vol. 57, no. 5, pp. 400–409, May 2008.

[23] A. Pavlov and N. van de Wouw, "Convergent systems: Nonlinear simplicity," in *Nonlinear Systems*. Berlin, Germany: Springer, 2017, pp. 51–77.

[24] A. Pavlov, N. van de Wouw, and H. Nijmeijer, "Frequency response functions for nonlinear convergent systems," *IEEE Trans. Autom. Control*, vol. 52, no. 6, pp. 1159–1165, Jun. 2007.

[25] A. Pavlov, N. van de Wouw, and H. Nijmeijer, "Global nonlinear output regulation: Convergence-based controller design," *Automatica*, vol. 43, no. 3, pp. 456–463, Mar. 2007.

[26] A. V. Pavlov, N. van De Wouw, and H. Nijmeijer, "Convergent systems: Analysis and synthesis," in *Control and Observer Design for Nonlinear Finite and Infinite Dimensional Systems*. Berlin, Germany: Springer, 2005, pp. 131–146.

[27] A. V. Pavlov, N. van De Wouw, and H. Nijmeijer, *Uniform Output Regulation of Nonlinear Systems: A Convergent Dynamics Approach*. Boston, MA, USA: Birkhäuser, 2006.

[28] R. Pintelon and J. Schoukens, *System Identification: A Frequency Domain Approach*. Hoboken, NJ, USA: Wiley, Mar. 2012.

[29] J. Reinders, D. Elshove, B. Hunnekens, N. van de Wouw, and T. Oomen, "Triggered repetitive control: Application to mechanically ventilated patients," *IEEE Trans. Control Syst. Technol.*, early access, Jan. 24, 2023, doi: 10.1109/TCST.2023.3237610.

[30] J. Reinders, B. Hunnekens, F. Heck, T. Oomen, and N. van de Wouw, "Accurate pressure tracking to support mechanically ventilated patients using an estimated nonlinear hose model and delay compensation," *Control Eng. Pract.*, vol. 106, Jan. 2021, Art. no. 104660.

[31] J. Reinders, B. Hunnekens, F. Heck, T. Oomen, and N. van de Wouw, "Adaptive control for mechanical ventilation for improved pressure support," *IEEE Trans. Control Syst. Technol.*, vol. 29, no. 1, pp. 180–193, Jan. 2021.

[32] J. Reinders, R. Verkade, B. Hunnekens, N. van de Wouw, and T. Oomen, "Improving mechanical ventilation for patient care through repetitive control," in *Proc. IFAC 21st Triennial World Congr.*, Berlin, Germany, Jul. 2020, pp. 1441–1446.

[33] B. S. Rüffer, N. van de Wouw, and M. Mueller, "Convergent systems vs. incremental stability," *Syst. Control Lett.*, vol. 62, no. 3, pp. 277–285, Mar. 2013.

[34] M. Scheel, A. Berndt, and O. Simanski, "Iterative learning control: An example for mechanical ventilated patients," *IFAC-PapersOnLine*, vol. 48, no. 20, pp. 523–527, 2015.

[35] M. Tomizuka, T.-C. Tsao, and K.-K. Chew, "Discrete-time domain analysis and synthesis of repetitive controllers," in *Proc. Amer. Control Conf.*, Atlanta, GA, USA, Jun. 1988, pp. 860–866.

[36] M. Tomizuka, T.-C. Tsao, and K.-K. Chew, "Analysis and synthesis of discrete-time repetitive controllers," *ASME J. Dyn. Syst., Meas., Control*, vol. 111, no. 3, pp. 353–358, Sep. 1989.

[37] C. M. Verrelli, "Adaptive learning control design for robotic manipulators driven by permanent magnet synchronous motors," *Int. J. Control*, vol. 84, no. 6, pp. 1024–1030, Jun. 2011.

[38] C. M. Verrelli, "PI-generalizing saturated repetitive learning control for a class of nonlinear uncertain systems: Robustness w.r.t. relative degree zero or one," *Syst. Control Lett.*, vol. 164, Jun. 2022, Art. no. 105248.

[39] C. M. Verrelli, S. Pirozzi, P. Tomei, and C. Natale, "Linear repetitive learning controls for robotic manipulators by Padé approximants," *IEEE Trans. Control Syst. Technol.*, vol. 23, no. 5, pp. 2063–2070, Sep. 2015.

[40] M. A. Warner and B. Patel, "Mechanical ventilation," in *Benumof and Hagberg's Airway Management*. Amsterdam, The Netherlands: Elsevier, 2013, pp. 981–997.

[41] V. Yakubovich, "Matrix inequalities method in stability theory for nonlinear control systems: I. Absolute stability of forced vibrations," *Automat. Remote Control*, vol. 7, nos. 905–917, p. 202, 1964.